

Evaluating the Robustness of Global Appearance Descriptors in a Visual Localization Task, under Changing Lighting Conditions

Vicente Román, Luis Payá and Óscar Reinoso

Engineering Systems and Automation Department, Miguel Hernandez University, Elche (Alicante), Spain

Keywords: Mobile Robots, Global Appearance Descriptors, Omnidirectional Images, Mapping, Localization.

Abstract: Map building and localization are two important abilities that autonomous mobile robots must develop. This way, much research has been carried out on these topics, and researchers have proposed many approaches to address these problems. This work presents some possibilities to solve these problems robustly using global appearance descriptors. In this way, robots capture visual information from the environment and obtain, usually by means of a transformation, a global appearance description for each whole image. Using these descriptors, the robot is able to estimate its position in a previously built map, which is also composed of a set of global appearance descriptors. In this work, the global appearance descriptors performance at the localization task inside a known environment has been studied. In the assignment a map is already built and the goal is to evaluate the descriptors' robustness to perform localization tasks when the environment visual appearance changes substantially. To achieve this objective, a comparative evaluation of several global appearance descriptors is carried out.

1 INTRODUCTION

Over the last few years, the presence of mobile robots in industrial and domestic environments has increased substantially. This increase has been facilitated by the development of their abilities in perception and computation, which allow them to improve the operation in large and heterogeneous areas without the necessity of introducing changes into the robot or environment structure. However, the mobile robot boom will not be definitive until the level of autonomy and the adaptability to different conditions enhance substantially. An autonomous robot has to find a good solution to two critical problems: building a model of the environment (mapping) and estimating the position of the robot within this model (localization). Both have to be solved with an acceptable accuracy and computational cost.

Nowadays, one of the most extended systems to obtain information from the environment are vision sensors, which permit extracting local information from the scenes. The use of local appearance descriptors has been the classical approach for obtaining relevant information from the images. This is a mature and very developed alternative and many researchers make use of it in mapping and localization. For example Valgren and Lilienthal (Valgren and Lilienthal,

2010) have proposed using these descriptors to perform topological localization. Murillo et al. (Murillo et al., 2007) present a comparative study for the localization task in indoor environments. A comparative evaluation of this kind of local appearance methods was made by Gil et al. (Gil et al., 2010). In this paper they evaluated, the repeatability of these detectors, as well as the invariance and distinctiveness of the descriptors under different perceptual conditions. More recently, an alternative has emerged, which consists in representing each image as a whole, without extracting local features. This method could offer comparative results and it also simplifies the structure of the map. Additionally, localization can be carried out with a simple process, based on the pairwise comparison of global descriptors. As a disadvantage, it has to work a large amount of data, so is necessary to use a compression technique that minimize the computational cost.

Some researchers have proposed different methods to describe the global appearance of the scenes, which maintain the necessary information to do the localization and mapping tasks. The discrete Fourier Transform is one alternative. (Menegatti et al., 2004) submit the Fourier Signature (FS) concept and define a method to carry out mapping and localization. Other studies support a method based on the Histogram of

Oriented Gradients (HOG). For example (Dalal and Triggs, 2005) use this method to detect pedestrians with a good performance and (Payá et al., 2016) prove the robustness of the descriptor in mapping and localization tasks. Furthermore, a method known as gist, which tries to imitate the human vision system, can be used. Oliva and Torralba were precursors of this idea (Oliva and Torralba, 2001). Other authors, like Siagian and Itti, have used this method in their work (Siagian and Itti, 2009) where they have described this biological inspired vision localization system and have tested it in different outdoor environments. Finally, the Radon Transform could be used to compress the information too, as (Berenguer et al., 2016) show in their studies.

In our experiments we use omnidirectional images, which give a 360 range vision so they offer more information than other visual systems. With this system, features are more time in the camera range vision so it allows to obtain stabler ones. Moreover, omnidirectional systems contains information enough to create a model if a person or an object occlude the image during the route.

In this area, previously works like (Payá et al., 2016) present a comparative evaluation of these global-appearance techniques in topological mapping tasks. (Payá et al., 2017) present an evaluation of these descriptors in compacting visual maps using FS, HOG and gist descriptors. The goal of this paper is to extend these previous works. On the one hand, we include a new scene descriptor called Radon transform and; on the other hand, we compare the methods on a real and changing environment.

We have studied the global-appearance descriptors strength, verifying their performance when the environment visual appearance changes substantially. In real-operating conditions the robot has to cope with different events: not the same lighting conditions between the model and the new localization; scenes occluded by people or other mobile robots and changes in the scene like the furniture position.

2 REVIEW OF GLOBAL APPEARANCE DESCRIPTORS

In this section we summarize some alternatives to extract global information from panoramic images trying to keep relevant data with the minimum memory. As the images used in this work are given in an omnidirectional form, the first step is to transform them into a panoramic ones. This process is fairly slow and it will affect to the computational cost. The starting point is a panoramic image $i(x,y) \in \mathbb{R}^{N_x \times N_y}$ and after

using the global appearance method the result is a descriptor $\vec{d} \in \mathbb{R}^{l \times 1}$.

The robot has a planar movement and to capture the images a catadioptric vision system is used (Pronobis and Caputo, 2009). This system is mounted vertically on a robot, a camera and a convex mirror were aligned and mounted together on a portable bracket to build the vision system. The movement of this robot is restricted to the floor plane.

2.1 Fourier Signature

(Menegatti et al., 2004) show that when we calculate the Discrete Fourier Transform of each row of a panoramic image $f(x,y)$, we obtain a new complex matrix $\mathbf{F}(u,v)$ that can be split in two matrices: one with the modules $\mathbf{A}(u,v)$ and other with the arguments $\Phi(u,v)$.

Two images that have been taken from the same position but with different orientation would have the same modules' matrix but a change in the arguments' matrix is produced, according to the shift property of the Fourier Transform. The relative rotation between images could be calculated (Payá et al., 2009). So we can use $\mathbf{A}(u,v)$ as a localization descriptor and $\Phi(u,v)$ as an orientation estimator.

Furthermore, in the Fourier domain, the most relevant information is concentrated in the low frequency components so we can discard a number of high frequency components that are usually affected by noise. It allows us to minimize the computational cost in the subsequent comparisons. In this work we use the parameter k_1 which indicates the number of frequencies we retain. N_x is the panoramic image number of rows. The image is reduced into a global appearance descriptor $\vec{d} \in \mathbb{R}^{N_x \cdot k_1 \times 1}$.

2.2 Histogram of Oriented Gradient

As (Dalal and Triggs, 2005) describes, the HOG technique works with the orientation of the gradient in specific areas. Hofmeister et al. use a weighted histogram of oriented gradients in small and controlled environments (Hofmeister et al., 2009).

Essentially it consists in calculating the gradient of the panoramic image obtaining module and orientation of each pixel to localize mobile robots. Afterwards, the image is divided in a set of cells and the orientation histogram of each cell is calculated, weighting the each bin with the module of the gradient of each pixel. Although the image is rotated, two panoramic images contain the same information in each row, but a shift of the pixels. As a result, if we divide the image into horizontal cells, a descriptor

will be obtained which is invariant to rotations of the robot in the floor plane and can be used as a localization descriptor.

Moreover, the whole image can be reduced to a vector whose size will depend on the number of cells and bins. In this work we use b_1 , which is the number of bins per histogram and k_2 , which is the number of horizontal cells in which the image has been divided. This method transform the panoramic image into a descriptor $\vec{d} \in \mathbb{R}^{b_1 \cdot k_2 \times 1}$.

2.3 Gist

This descriptor was initially described in (Oliva and Torralba, 2006), and further developed in other studies like (Siagian and Itti, 2009) where gist descriptor had been tested in three outdoor environments.

The method offers rotational invariance when it is applied to panoramic images. The descriptor is built from orientation information, obtained after exposing some Gabor filters with different orientations to the image in several resolution levels. Finally, the volume of data is reduced for an average; like when we use HOG, we divide the image with horizontal cells and we calculate the mean intensity of each cell.

On this way, we use m_1 which indicates the number of orientations of Gabor filters and k_3 that designates the number of horizontal cells in which the image has been split. With these parameters the image can be reduced to a descriptor whose size depends on m_1 , k_3 and the number of different resolution models used, but in the experiments we maintain this parameter constant in 2 levels. So finally the result is a global appearance descriptor $\vec{d} \in \mathbb{R}^{2 \cdot m_1 \cdot k_3 \times 1}$.

2.4 Radon Transform

The Radon Transform can also be used to describe globally an omnidirectional image. This transformation was described in (Radon, 2005). It was used in some computer vision activities, such as (Hoang and Tabbone, 2010) where the Radon transform (RT) was used as a geometric shape descriptor. In the robotic field we can find the study (Berenguer et al., 2016) where RT was employed to find the nearest neighbor in a position estimation.

Radon method can be used directly with omnidirectional images so they have not to be transformed into panoramic. It will presume a reduction in the computational cost. The method consists in applying the Radon Transform along several sets of straight lines, with a variety of orientations between consecutive sets. The difference of orientation is considered a variable parameter named p_1 (deg.). This way, an

omnidirectional image data can be transformed to a vector that fulfills some interesting properties. (a) It reduces the information; figure 1 shows an image $N_x \times N_x$ which could be reduced into a $\frac{360}{p_1} \times 0.5 \cdot N_x$ matrix; (b) invariability of the information if against changes of the robot orientation and (c) possibility of calculate the orientation with a column shift.

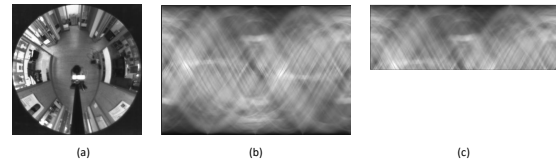


Figure 1: Radon transform. (a) omnidirectional image ($N_x \times N_x$). (b) Radon transform of a the image ($\frac{360}{p_1} \times N_x$) and (c) final Radon transform ($\frac{360}{p_1} \times 0.5 \cdot N_x$).

When the Radon transform has been calculated, the localization process could be addressed with some methods. In this paper we use a method based on FS. We apply the Fourier Signature to transform the data we obtain after we have calculated the Radon Transform. We get two matrices (magnitudes and arguments) and the descriptors are built as described in section 2.1.

In this case, the descriptor size will depend on p_1 and the number of columns we retain once we apply the FS. This parameter is called k_4 . The descriptor obtained is $\vec{d} \in \mathbb{R}^{\frac{360}{p_1} \cdot 0.5 \cdot N_x \times 1}$.

3 SETS OF IMAGES

In this work, the COLD database (Pronobis and Caputo, 2009) is used. This database provides omnidirectional image sequences taken under three different lighting conditions: a sunny day, a cloudy one and at night. The images were acquired across several days under illumination variations as well as changes introduced by human activity in the environment (people appearing in the rooms, objects and furniture being relocated or moved and so on). These different conditions can be seen in figure 2

Therefore, the COLD database is an ideal test bench to evaluate the localization and mapping algorithms' robustness because it offers variations that might occur in real-world environments. COLD database offers diverse routes captured in indoor environments in several universities. Among those possibilities we use Freiburg dataset and the longest route, called Part A, Path 2, size 3 (Pronobis and Caputo, 2009). Freiburg route supposes an especial challenging one because many walls between rooms are made of glass and there are lots of windows so the extern



(a) Image from the sunny dataset



(b) Image from the night dataset

Figure 2: Panoramic images from COLD database.

light conditions affect substantially the localization task.

The sequences of this set of images were recorded using a mobile robot and both perspective and omnidirectional cameras. The catadioptric vision system was made using a hyperbolic mirror was mounted with the cameras on a portable bracket. The robot was also equipped with a laser range scan and wheels encoders to detect the odometry.

4 EXPERIMENTS

In this section we test the global-appearance descriptors effectiveness. First we outline the distances and measurement error models used, then we present the localization results considering different illumination (Cloudy weather, sunny weather and at night) and the computational cost of these experiments.

4.1 Method to Create a Model of the Environment

As explained in the previous section, COLD offers different databases captured in diverse buildings and conditions. We use Freiburg cloudy dataset to build the model. COLD database took an image every 0.06m approximately. To build our model we make a reduction taking one every five images, so our model follow the same route but the distance between images is around 0.30m. This method allows us to have a model with 556 images instead of 2778 images that cloudy dataset (Part A, Path 2, size 3) have.

Once we have built the model with known images, the method to solve the localization task consists in comparing each image from a test group with the images in the model. The program calculates the nearest neighbor. To obtain the nearest neighbor different distances can be used. In our study we compare

Table 1: Distances.

Measure	Distance	Mathematical expression
d1	Cityblock	$d_1(\vec{a}, \vec{b}) = \sum_{i=1}^l a_i - b_i $
d2	Euclidean	$d_2(\vec{a}, \vec{b}) = \sqrt{\sum_{i=1}^l (a_i - b_i)^2}$
d3	Correlation	$d_3(\vec{a}, \vec{b}) = 1 - \frac{\vec{a}_d^T \cdot \vec{b}_d}{ \vec{a}_d \cdot \vec{b}_d }$
d4	Cosine	$d_4(\vec{a}, \vec{b}) = 1 - \frac{\vec{a}^T \cdot \vec{b}}{ \vec{a} \cdot \vec{b} }$

Where:

$$\vec{a}_d = [a_1 - \bar{a}, \dots, a_l - \bar{a}]; \bar{a} = \frac{1}{l} \cdot \sum_j a_j$$

$$\vec{b}_d = [b_1 - \bar{b}, \dots, b_l - \bar{b}]; \bar{b} = \frac{1}{l} \cdot \sum_j b_j$$

these ones: *cityblock*, *Euclidean*, *correlation* and *cosine*. Table 1 shows the definition of each distance. At the mathematical expression, $\vec{a} \in \mathbb{R}^{l \times 1}$ and $\vec{b} \in \mathbb{R}^{l \times 1}$ are two vectors where: $a_i, b_i, i = 1, \dots, l$.

Once the nearest neighbor is obtained we calculate the geometric distance between the test image and his neighbor, and the result will be the error. This real distance can be calculated because COLD database offers the coordinates where each image had been captured but the coordinates have been only used as ground truth to check the error. The localization task is carried out with pure visual information.

The experiments have been done using different descriptors and varying the parameters that could be modified in order to evaluate the influence of each parameter in the task. These parameters can be seen in table 2. As shown in section 2, these parameters define the descriptor size. The larger the descriptor is, the slower the process will be.

Table 2: Parameters that impact on the location process.

Descriptor	Parameters
FS	$k_1 \Rightarrow$ number of retained columns.
HOG	$b_1 \Rightarrow$ number of bins per histogram.
	$k_2 \Rightarrow$ number of horizontal cells.
gist	$m_1 \Rightarrow$ number of Gabor filters.
	$k_3 \Rightarrow$ number of horizontal blocks.
Radon	$p_1 \Rightarrow$ degrees between sets of lines.
	$k_4 \Rightarrow$ number of retained columns.

4.2 Position Estimation

Initially, the cloudy images are used to create the reference model. Afterwards, to study the robustness of the global-appearance descriptors, the test images used to solve the localization problem will be chosen from the sunny and night datasets, which are composed of 2231 and 2896 images, respectively. The localization process evaluates which image in the reference model is the most similar to each test image. The error is calculated as the geometric distance between the capture points of both images. After re-

peating this process considering all the sunny images as test image, figures 3, 4, 5 and 6 show the average error (m) with each descriptor method.

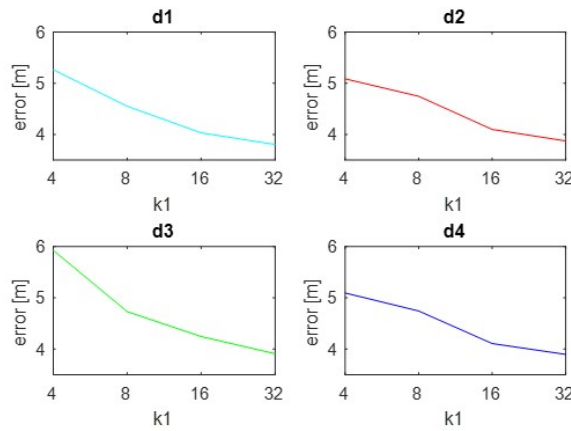


Figure 3: FS. Localization error (m) using test images from the sunny dataset versus k_1 .

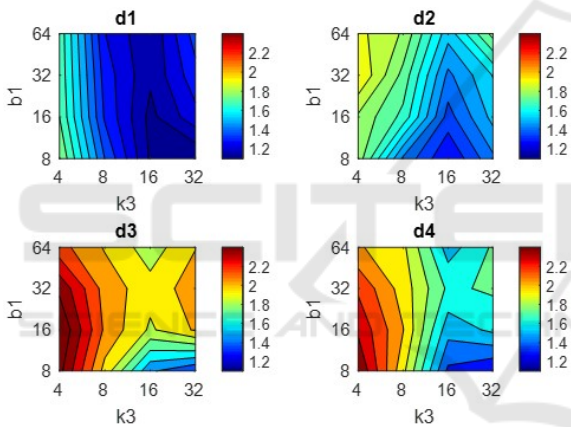


Figure 4: HOG. Localization error (m) using test images from the sunny dataset versus k_2 and b_1 .

The behaviour of the FS changes depending on the distance measure used, although d_2 and d_4 offer similar results. The error varies between 3 and 7 meters. The higher k_1 is, the better results we obtain but the process will be slower. We obtain the best accuracy with d_3 and $k_1=128$ where the location error is 3,56m; when $k_1=32$ the error is 3,91m.

About HOG, a medium-high value of k_2 and an intermediate value of b_1 offer the best results. The lowest error is obtained using distance d_1 and $b_1=32$ and $k_2=8$ and it is 1,09m.

In general, using the gist descriptor, the error is about 2m. The error decreases with medium values of k_3 and medium-low values of m_1 . The best solution is detected with d_3 and $k_3=m_1=16$ where the error is 1,69m.

At last, in the case of RT, the results are in general worse. The error is higher than 5m in most cases. The

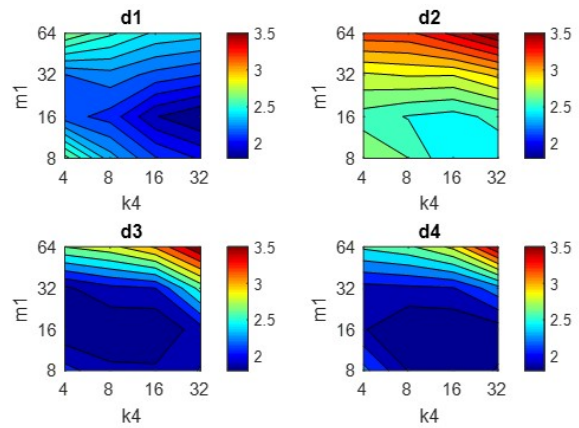


Figure 5: gist. Localization error (m) using test images from the sunny dataset versus k_3 and m_1 .

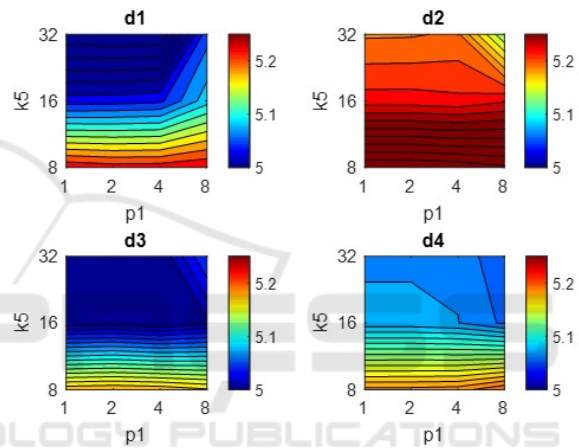


Figure 6: Radon. Localization error (m) using test images from the sunny dataset versus p_1 and k_4 .

error depends more on the k_4 parameter and the higher it is, the lower the error is. The lowest error is detected when $k_4=32$ and $p_1=1$. With these parameters and d_1 the error is 4,93m.

Analysing globally these figures, HOG and gist are the description algorithms with a lower error that varies between 1 and 2 m when they use d_1 and d_3 . There are remarkably good results taking into account that not only the illumination changes, but also furniture movements and occlusions appear in the scenes.

After this experiment, the localization process is repeated considering all the images in the night set as test images. Like in the previous case, the reference model is precisely created with cloudy images. Figures 7, 8, 9 and 10 present the results showing the error in meters.

The results using FS are between 0,6 and 2,5m. Low values of k_1 offer lower errors, obtaining the best one with $k_1=4$ and distance d_1 where the error is 0,597m.

The behaviour with HOG presents an error be-

tween 0,2 and 0,6m . The best results are given with intermediate values of k_2 and b_1 and the distance $d1$. With $k_2=32$, $b_1=16$ and distance $d1$ we obtain the lowest error, 0,189m.

About gist, the mean error is between 0,2 and 1m. If k_3 or m_1 values are low, the error will increase and it will not decrease significantly when the parameters are high. In fact it will offer relatively bad results if m_1 increases a lot; so medium values are the best choice. The lowest error has been obtained with the distance $d1$, $k_3=32$ and $b_1=8$, when the error is 0,21m. The maximum error in our night proofs using gist has been 1,37m. It has been obtained with $d3$, $k_4=2$ and $m_1=256$. This is a relatively low error if it is compared with the maximum error using other descriptors.

Finally, the localization error with Radon is between 0,4 and 1,8m. The lower k_4 is, the lower the error is; p_1 has little influence in the results. When $k_4=32$, $p_1=1$ and $d3$ the localization error is 0,3281m.

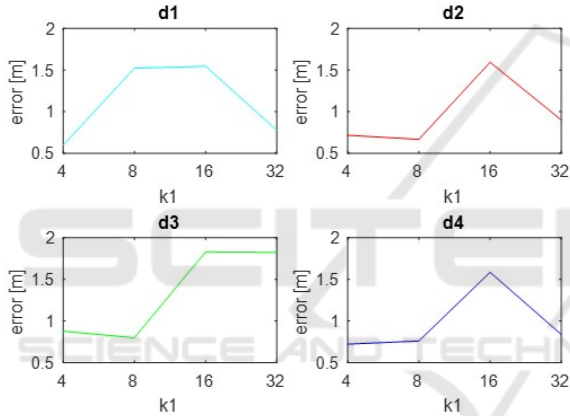


Figure 7: FS. Localization error (m) using test images from the **night** dataset versus k_1 .

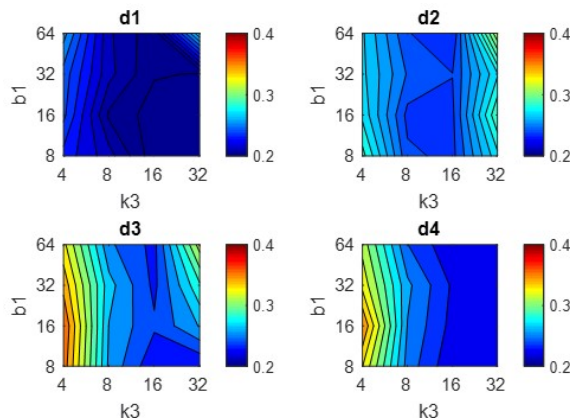


Figure 8: HOG. Localization error (m) using test images from the **night** dataset versus k_2 and b_1 .

It is remarkable that we obtain better results when the localization task is made at night than when it was made on a sunny day. This could be cause because of

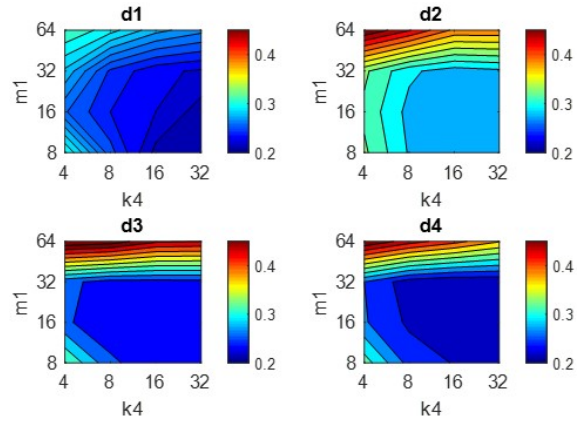


Figure 9: Gist. Localization error (m) using test images from the **night** dataset versus k_3 and m_1 .

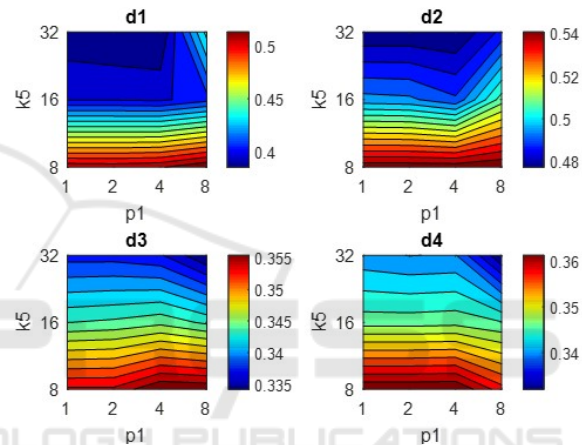


Figure 10: Radon. Localization error (m) using test images from the **night** dataset versus p_1 and k_4 .

the large amount of walls made of by glass in Freiburg database; and, as we work with different lighting conditions, it could cause anomalies, such as brights and reflections. But taking into account the great challenge that it suppose, the localization presents notably good results in both states.

4.3 Computational Cost

Besides having a low error, it is important to have a reasonable computation time. We have also studied the computational time the process spends in order to know if the localization can be made in real time. Figures 11, 12, 13 and 14 show the runtime needed to estimate the robot position with each descriptor method and distance measure. The data are given in seconds.

FS offers the quickest results. The highest time is 0,221s when $k_1=32$ and the distance $d3$. The time has an exponential growth when the variable k_1 increases.

Runtimes with HOG are similar to FS ones. The optimal result is 0.235s. When the parameters in-

crease, the runtime increases too. b_1 has more influence so it is important not to have high values of it. However, k_2 has less importance in the runtime.

Gist does not offer a quick runtime if it is compared with other descriptors. Using gist the runtime could be 0,537s when $m_1=64$ and $k_3=32$. In this case, the parameter m_1 has a lot of importance in the time. The quickest runtime with gist is given when $m_1=8$ and $k_3=4$, whose associated time is 0.2405s.

Finally, we have studied the RT runtime. We can observe high dependence on p_1 and less importance of k_4 . The lower p_1 , is the higher the runtime will be. The highest time is 0,447s with $p_1=1$ and $k_4=16$ but Radon could offer relatively reduced times like 0.059s when $p_1=8$ and $k_4=4$.

The time spent while the program had to change from omnidirectional images to panoramic ones is the time which has more relevance in the results obtained. So the compression process and the comparison between descriptors have less importance. As a result the experiments give us similar runtimes between Fourier and HOG and a slow runtime with gist. The RT process does not have to change the images to panoramic pictures so it reduces the cost of the process, but when p_1 is low, its compression process is slower and it has significant relevance in the RT process. The experiments have been carried out in a PC with a CPU Quad-Core Intel i7-700® at 3.60 GHz and through Matlab® programming.

These results are not absolute, they will depend of the machine which runs the process. But they are comparable because all the calculations have been done with the same computer.

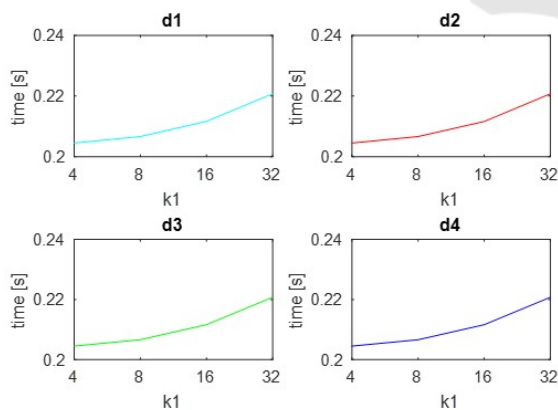


Figure 11: FS. Localization time (s) per image versus k_1 .

5 CONCLUSIONS

This work has focused on the study of different problems in navigation tasks under illumination variations

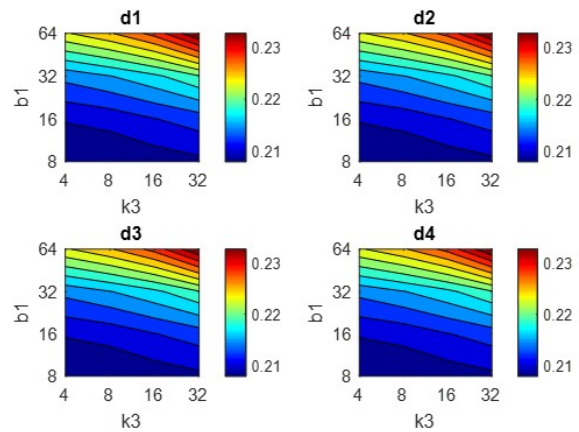


Figure 12: HOG. Localization time (s) per image versus k_2 and b_1 .

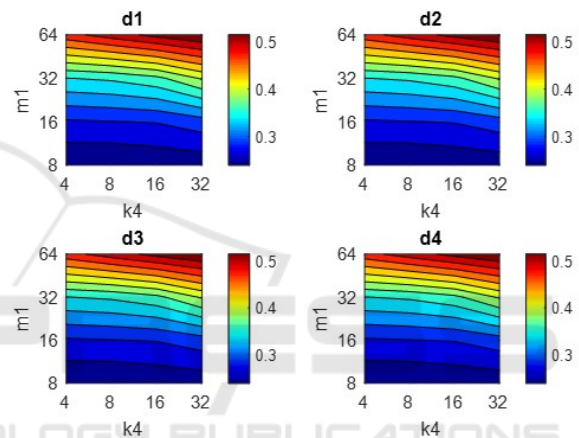


Figure 13: gist. Localization time (s) per image versus k_3 and m_1 .

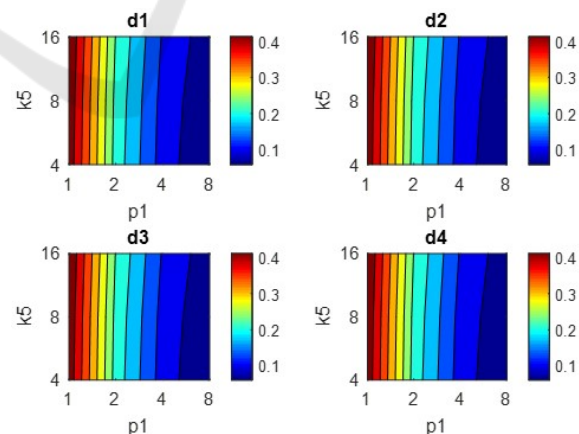


Figure 14: Radon. Localization time (s) per image versus p_1 and k_4 .

and changes introduced by human activity, and the robot is only equipped with an omnidirectional camera. We have compared four appearance-based algorithms applied to this localization task. When the im-

ages have been described and the localization error has been calculated a comparative evaluation has been carried out and the computational cost has also been studied.

On the one hand, the Fourier Signature and HOG offer quicker results, so they constitute the most suitable option to do tasks in real time. On the other hand, HOG and gist descriptors provide better accuracy in localization tasks.

This work opens the door to new applications of the appearance-based methods in mobile robots. As we have shown, the appearance-based descriptors are a suitable method to do navigation tasks. A problem is the high requirements of memory and computation time to do the database and make the necessary calculations to compute the position. Once we have tested the methods' robustness under human activity and changes in illumination and in the position of some objects, the next step should be to create a method that continuously renews the database adapting it to new lighting conditions. It can also evolve to a system that creates more sophisticated maps to make it possible an autonomous navigation system.

ACKNOWLEDGEMENTS

This work has been supported by the Spanish Government through the project DPI 2016-78361-R (AEI/FEDER, UE): "Creación de mapas mediante métodos de apariencia visual para la navegación de robots".

REFERENCES

- Berenguer, Y., Payá, L., Peidró, A., Gil, A., and Reinoso, O. (2016). Nearest position estimation using omnidirectional images and global appearance descriptors. In *Robot 2015: Second Iberian Robotics Conference*, pages 517–529. Springer.
- Dalal, N. and Triggs, B. (2005). Histograms of oriented gradients for human detection. In *2005 IEEE Computer Society Conference on Computer Vision and Pattern Recognition (CVPR'05)*, volume 1, pages 886–893 vol. 1.
- Gil, A., Mozos, O. M., Ballesta, M., and Reinoso, O. (2010). A comparative evaluation of interest point detectors and local descriptors for visual slam. *Machine Vision and Applications*, 21(6):905–920.
- Hoang, T. V. and Tabbone, S. (2010). A geometric invariant shape descriptor based on the radon, fourier, and mellin transforms. In *Pattern Recognition (ICPR), 2010 20th International Conference on*, pages 2085–2088. IEEE.
- Hofmeister, M., Liebsch, M., and Zell, A. (2009). Visual self-localization for small mobile robots with weighted gradient orientation histograms. In *40th International Symposium on Robotics (ISR)*, pages 87–91. Barcelona.
- Menegatti, E., Maeda, T., and Ishiguro, H. (2004). Image-based memory for robot navigation using properties of omnidirectional images. *Robotics and Autonomous Systems*, 47(4):251 – 267.
- Murillo, A. C., Guerrero, J. J., and Sagues, C. (2007). Surf features for efficient robot localization with omnidirectional images. In *Robotics and Automation, 2007 IEEE International Conference on*, pages 3901–3907. IEEE.
- Oliva, A. and Torralba, A. (2001). Modeling the shape of the scene: A holistic representation of the spatial envelope. *International journal of computer vision*, 42(3):145–175.
- Oliva, A. and Torralba, A. (2006). Building the gist of a scene: The role of global image features in recognition. *Progress in brain research*, 155:23–36.
- Payá, L., Fernández, L., Reinoso, Ó., Gil, A., and Úbeda, D. (2009). Appearance-based dense maps creation-comparison of compression techniques with panoramic images. In *ICINCO-RA*, pages 250–255.
- Payá, L., Mayol, W., Cebollada, S., and Reinoso, O. (2017). Compression of topological models and localization using the global appearance of visual information. In *Robotics and Automation (ICRA), 2017 IEEE International Conference on*, pages 5630–5637. IEEE.
- Payá, L., Reinoso, O., Berenguer, Y., and Úbeda, D. (2016). Using omnidirectional vision to create a model of the environment: A comparative evaluation of global appearance descriptors. *Journal of Sensors*, 2016.
- Pronobis, A. and Caputo, B. (2009). COLD: COsy Localization Database. *The International Journal of Robotics Research (IJRR)*, 28(5):588–594.
- Radon, J. (2005). 1.1 über die bestimmung von funktionen durch ihre integralwerte längs gewisser mannigfaltigkeiten. *Classic papers in modern diagnostic radiology*, 5:21.
- Siagian, C. and Itti, L. (2009). Biologically inspired mobile robot vision localization. *IEEE Transactions on Robotics*, 25(4):861–873.
- Valgren, C. and Lilienthal, A. J. (2010). Sift, surf & seasons: Appearance-based long-term localization in outdoor environments. *Robotics and Autonomous Systems*, 58(2):149–156.